Discrimination of basmati and non-basmati rice types using polarimetric target decomposition of temporal SAR data

Vineet Kumar[1], Mamta Kumari[2,*] and S. K. Saha[2]

[1]Indian Institute Technology Bombay, Powai, Mumbai 400 076, India
[2]Indian Institute of Remote Sensing (ISRO), 4, Kalidas Road, Dehradun 248 001, India

The present study distinguishes the growing areas of basmati and non-basmati rice types using polarimetric target decomposition technique on temporal Synthetic Aperture Radar (SAR) data. Multi-temporal quad-pol RADARSAT-2 data of part of the Indo-Gangetic plains were acquired to analyse the contribution of different scattering components (double bounce, singe bounce and volume scattering) at various crop growth stages of both rice types. A decision tree-based framework has been proposed to segregate both rice types and other major land use–land cover classes by capturing the temporal variations in different scattering components. Both rice types were separated in the study area with user's accuracy of 85.19% and 82.93% for non-basmati and basmati rice respectively.

Keywords: Basmati rice, decision-tree classifier, polarimetric target decomposition, Synthetic Aperture Radar.

THE timely information on rice acreage and growth status is important for an agricultural economy-based country like India, which shares 20% of global rice production. Basmati rice (aromatic) localized to the Indian subcontinent and known for its export quality generates three times higher price than non-basmati rice types. It is cultivated in the monsoon (*kharif*) season only[1]. Discrimination and mapping of basmati and non-basmati rice types play an important role in national economy. With the ability to provide continuous information in all-weather and day–night conditions, space-borne Synthetic Aperture Radar (SAR) systems are useful for the monitoring and mapping of *kharif* crops. Polarimetric SAR systems not only record mutually coherent, fully polarimetric information about the target, but also retain phase information during the processing. Polarimetric SAR data can further be interpreted using different target-based scattering mechanisms (double bounce, volume scattering and surface scattering) using polarimetric target decomposition techniques[2,3]. With the launch of fully polarimetric spaceborne SAR sensors like RADARSAT-2, ALOS/PALSAR and TERRA SAR-X, it is now possible to acquire information about physical and dielectric properties of targets in all the linear polarization modes (HH, HV, VH and VV). The target decomposition products of fully polarimetric SAR data have been efficiently utilized for mapping purpose of various land use–land cover (LULC) classes using decision tree-based object oriented analysis[4]. Researchers have efficiently utilized this potential of quad-pol SAR data in crop mapping and monitoring in cloudy conditions, especially for rice crop. Across different frequencies, the following aspects of rice crop have been addressed in different studies: (i) biophysical parameter estimation[5,6]; (ii) identification and classification with other crops[7] and (iii) time-series growth analysis[8,9] and backscatter modelling[10].

This study investigates the potential of quad-pol C-band SAR data to discriminate basmati (aromatic) and non-basmati rice types. For this, we have analysed the backscattering response using three-component polarimetric target decompositions for two rice varieties. Using the target decomposition analysis a decision rule-based framework was designed to explore the capability of multi-temporal quad-pol RDARASAT-2 data to segregate and map basmati and non-basmati rice types.

The present study was conducted in the part of Karnal district, Haryana, India, bounded between lat. 29°37′42″–29°56′19″N and long. 76°36′23″–76°56′40″E, with an elevation of 240 m amsl. As Karnal district is the part of the Indo-Gangetic plains, its land is plain, alluvial and productive for agriculture. Soil texture of the study area varies from sandy loam to clay loam (medium to heavy). Rice is a major *kharif* season crop; both basmati and non-basmati rice types are grown simultaneously in the study area. In the test area non-basmati rice was transplanted between 15 and 30 June and harvested during 5–15 October 2012. Due to low temperature requirement at ripening stage, basmati rice was transplanted slightly late (in the first week of July) and harvested between 25 October and 5 November 2012.

Four scenes of RADARAST-2 fine quad-pol single-look complex (SLC) were acquired over the study area. Table 1 shows the characteristics of the acquired scenes. RADARSAT-2 data processing steps involved radiometric calibration, multilooking, speckle filtering, polarimetric decomposition and co-registration of all four imageries. To reduce inherent speckle noise effect, multilooking and 5 × 5 window size refined LEE filter was applied on all images. Acquired scenes of RADARSAT-2 have shown a shift while performing automatic co-registration due to different pass modes (ascending and descending pass modes as shown in Table 1). Therefore, manual co-registrations were performed on all scenes.

Model-based polarimetric target decompositions were applied on coherency matrix [T_3] in PolSARpro_v4.2.0 on pre-processed images. Three-component physically model-based polarimetric incoherent target decomposition theorems, and Freeman–Durden three-component[2], Yamaguchi three-component[11], van Zyl three-component decompositions[12] were applied to understand rice scattering

*For correspondence. (e-mail: mamta9507@gmail.com)

Table 1. Temporal RADARSAT-2 scene characteristics with rice growth stages

	Scene characteristics		Rice growth stage	
Acquisition date	Pass/beam mode	Incidence angle (°)	Non-basmati	Basmati
12 July 2012	Ascending/FQ9	28.00–29.87	Early tillering	Just transplanted
10 August 2012	Descending/FQ16	35.46–37.02	Late tillering	Tillering
15 September 2012	Ascending/FQ15	34.41–36.01	Ear differentiation, milking and heading	Pruned before panicle initiation
14 October 2012	Descending/FQ10	29.16–30.90	Harvested	Ear differentiation and milking

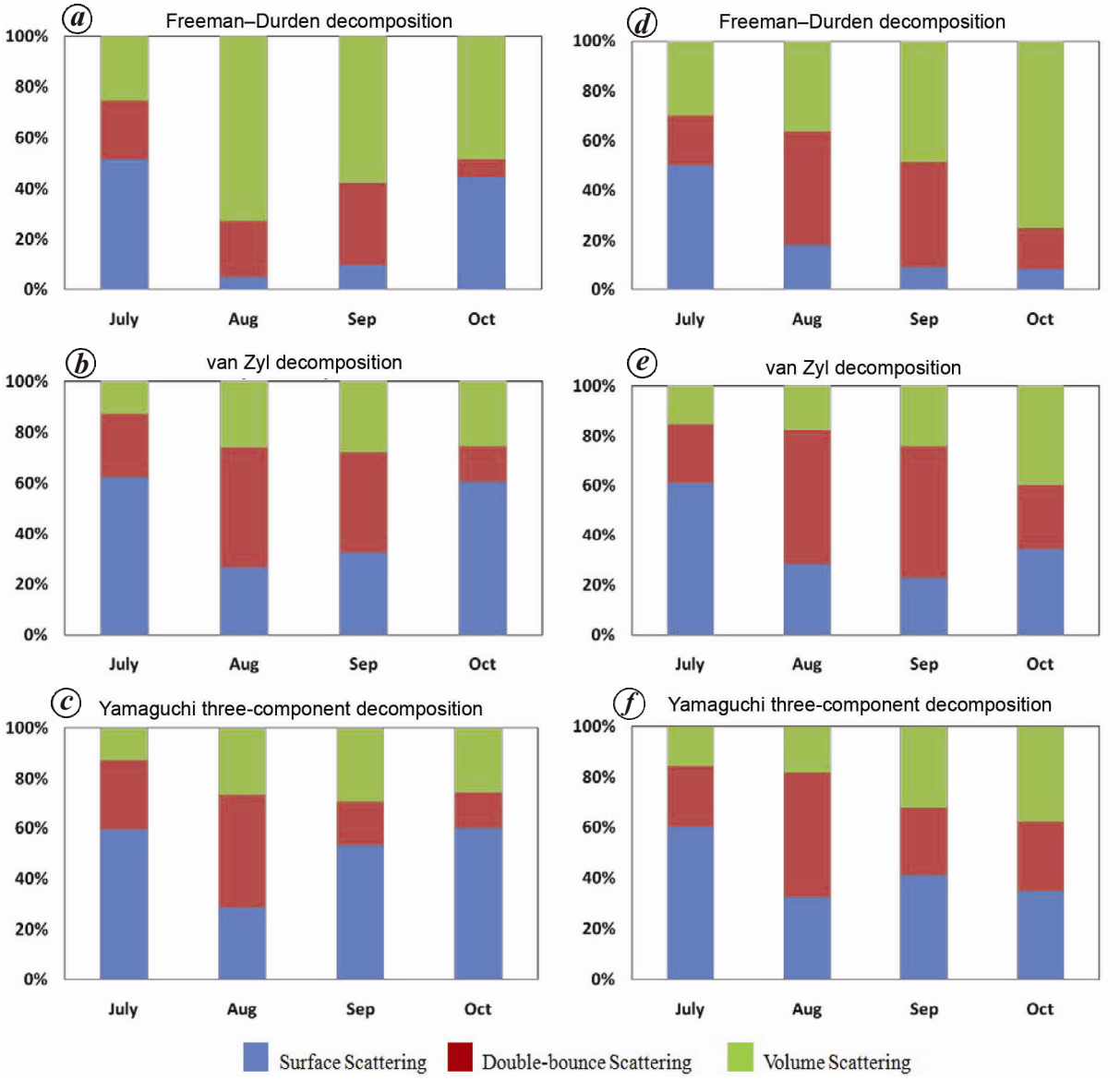

Figure 1. Graph showing temporal contribution of different scattering mechanisms by various decomposition techniques for (***a***–***c***) non-basmati rice and (***d***–***f***) basmati rice.

behaviour. These decompositions express the 3×3 coherency matrix $[T_3]$ as a weighted sum of three different scattering mechanisms, mainly surface scattering, double bounce and volume scattering. The first component of this decomposition considers Bragg's surface scatter model for slightly rough surfaces. The double-bounce scattering component was modelled by considering scattering from a dihedral corner reflector such as trunk–ground interaction

Table 2. Accuracy totals with overall accuracy 85% and kappa coefficient 0.79

Land use–land cover class	Reference total	Classified total	Number correct	Producer's accuracy (%)	User's accuracy (%)
Non-basmati	90	81	69	76.67	85.19
Basmati	114	123	102	89.47	82.93
Water body	27	30	27	100	90
Orchard	33	33	27	81.82	81.82
Settlement	36	33	30	83.33	90.91

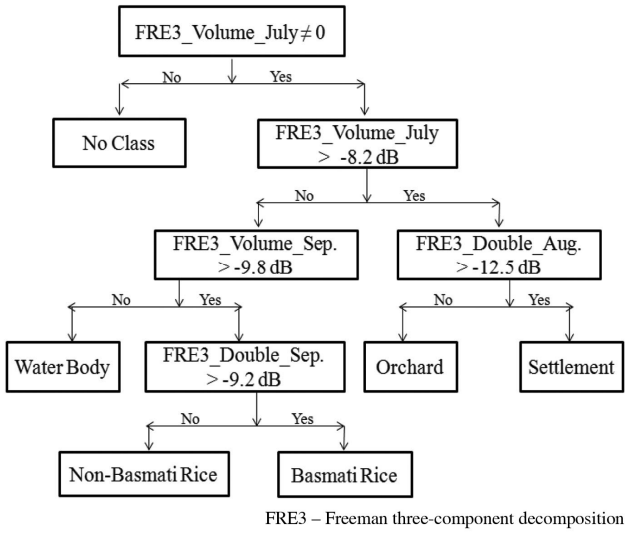

Figure 2. Decision rule-based framework for rice types and other major land use–land cover classes.

and volume scattering term was modelled as contribution from a cloud of randomly oriented cylinder-like scatterers. Scattering behaviour of the two rice types (basmati and non-basmati) was analysed temporally in the test site using these decomposition theorems.

Decision tree-based classifier was applied for crop discrimination at varietal level (basmati and non-basmati) using July–September SAR data. This classifier has discriminated rice types and other major land cover classes (orchard, water, settlement) on the basis of simple logic and mathematical rules applied on backscatter coefficient (σ_0) extracted from different scattering mechanisms (surface, double bounce and volume scattering) of Freeman three-component model-based decomposition.

Temporal contribution of three scattering mechanisms (odd bounce, double bounce, volume) from rice fields was analysed using Freeman, van Zyl and Yamaguchi target decompositions for both rice types. Figure 1 indicates relative percentage contribution of each scattering mechanism at different growth stages. Both basmati and non-basmati rice types are erectophile in nature, but basmati rice has narrow leaves and is taller than non-basmati rice, which results in weaker canopy structure of basmati rice (prone to lodging, more exposure of water background). In early growth stage (July) surface scattering (odd bounce) was the dominant scattering mechanism (>50% contribution) for both rice types. In August, the contribution of volume scattering component for non-basmati rice (approx 70%) and basmati rice (approx 30%) increased significantly in Freeman decomposition, while the other two decompositions indicated greater contribution by double-bounce scattering. However, the rate of increment of volume scattering component from July to August was higher for non-basmati rice than basmati rice due to more vegetative growth by early transplanting of the former one. In the test site, basmati rice was pruned in September to avoid lodging due to wind and rain; so the contribution of double-bounce scattering was comparatively higher for basmati rice (around 40% in Freeman decomposition and 60% in van Zyl decomposition) due to wave interaction with exposed water background and standing rice canopy. In October as non-basmati rice was harvested, the surface scattering was dominant with more than 40% contribution in all the decompositions. Basmati rice was still standing in the field with emerged ears, indicating dominance of volume scattering.

Among the three decomposition techniques used in this study, Freeman three-component decomposition was found predominantly separating the rice growth stages and rice types. So scattering component of this decomposition technique was used to classify rice types and other major land cover classes by decision tree algorithms (Figure 2). The other major LULC classes in the study area were orchard, settlements and water bodies. In July month, when rice was in its early growth stage, surface scattering was dominant from rice fields. Hence, higher mean value (> –8.2 dB) of volume scattering component of orchard and settlement pixels separated them from water bodies and rice field of study area. In September when both the rice types were in their full vegetative growth stage with high plant density, higher mean value (> –9.8 dB) of volume scattering corresponded to rice field pixels and separated it from water bodies. In September only basmati rice was pruned while in non-basmati ears emerged out in the test area; the double-bounce scattering at this stage discriminated the two rice types. Lower mean value (< –9.2 dB) of double-bounce component of September corresponds to non-basmati rice, while higher values correspond to basmati rice. In

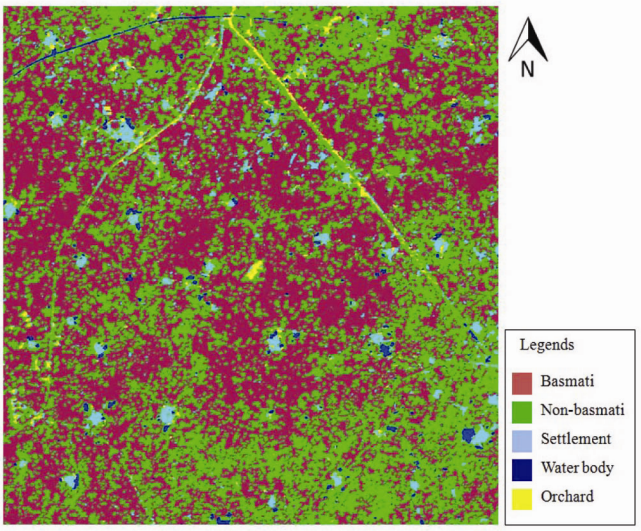

Figure 3. Classified output image showing spatial distribution of basmati and non-basmati rice types along with other major LULC classes in the study area.

August, double-bounce scattering component of Freeman decomposition further classified orchard and settlement pixels. The classification capability of the proposed decision-based algorithm was analysed by error matrix (Table 2) using ground-collected GPS information. The overall accuracy of the proposed method was found to be 85% with kappa coefficient of 0.79. User's accuracy (indicates commission error) of 85.19% and 82.93% was achieved for non-basmati and basmati rice types respectively (Table 2). As the basic crop structure of rice crop is the same, mixing of few pixels was observed within the rice types. Reasonable user's accuracy for water body (90%), orchard (81.82%) and settlement (90.91%) indicates the applicability of the proposed decision tree and scattering-based algorithm for other LULC classes. The settlements in the study area consist of rural housing along with open spaces and trees; hence mixing of this feature was observed with orchards. The classified output map of the study area (Figure 3) indicates the spatial distribution of basmati and non-basmati rice growing regions.

Due to delay in transplantation of basmati rice and the delayed onset of crop growth stages, differences in cultural practice and longer duration of basmati, it is possible to discriminate basmati and non-basmati rice types with a high level of accuracy. Contribution of each scattering component obtained by polarimetric target decomposition technique at different growth stages has clearly shown the difference in temporal profile of both rice types. The proposed framework indicates that multi-temporal decision-based classification scheme with the help of polarimetric target decomposition technique could provide spatial distribution of the two different rice types in the study area with reasonable accuracy.

1. Giraud, G., The world market of fragrant rice, main issues and perspectives. *Int. Food Agribus. Manage. Rev.*, 2013, **16**(2), 1–18.
2. Freeman, A. and Durden, S. L., A three component scattering model for polarimetric SAR. *IEEE Trans. Geosci. Remote Sensing*, 1998, **36**, 963–973.
3. Cloude, S. R. and Pottier, E., A review of target decomposition theorems in radar polarimetry. *IEEE Trans. Geosci. Remote Sensing*, 1996, **34**(2), 498–518.
4. Qi, Z., Anthony Gar-On Yeh, Li, X. and Lin, Z., A novel algorithm for land use and land cover classification using RADARSAT-2 polarimetric SAR data. *Remote Sensing Environ.*, 2012, **118**, 21–39; ISSN 0034-4257.
5. Inoue, Y., Sakaiya, E. and Wang, C., Capability of C-band backscattering coefficient from high resolution satellite SAR sensors to assess biophysical variables in paddy rice. *Remote Sensing Environ.*, 2014, **140**(214), 257–266.
6. Kumar, V., Kumari, M. and Saha, K. S., Leaf area index estimation of lowland rice using semi-empirical backscattering model. *J. Appl. Remote Sensing*, 2013, **7**(1), 073474–073484.
7. Shao, Y., Li, K., Touzi, R., Brisco, B. and Zhang, F., Rice scattering mechanism analysis and classification using polarimetric RADARSAT-2 data. In IEEE International Geoscience and Remote Sensing Symposium, 2012.
8. Yonezawa, C., Negishi, M., Azuma, K., Watanabe, M., Ishitsuka, N., Ogawa, S. and Saito, G., Growth monitoring and classification of rice fields using multitemporal RADARSAT-2 full-polarimetric data. *Int. J. Remote Sensing*, 2012, **33**(18), 5696–5711.
9. Chakraborty, M., Manjunath, K. R., Panigrahy, S., Kundu, N. and Parihar, J. S., Rice crop parameter retrieval using multi-temporal, multi-incidence angle Radarsat SAR data. *ISPRS J. Photogramm. Remote Sensing*, 2005, **59**(5), 310–322.
10. Wang, C., Wu, J., Zhang, Y., Pan, G., Qi, J. and Salas, W. A., Characterizing L-band scattering of paddy rice in Southeast China with radiative transfer model and multitemporal ALOS/PALSAR imagery. *IEEE Trans. Geosci. Remote Sensing*, 2009, **47**(4), 988–998.
11. Yamaguchi, Y., Moriyama, T., Ishido, M. and Yamada, H., Four component scattering model for polarimetric SAR decompositions. *IEEE Trans. Geosci. Remote Sensing*, 2005, **43**(8), 1699–1706.
12. van Zyl, J. J., Application of Cloude's target decomposition theorem to polarimetric imaging radar data. In San Diego 92, International Society for Optics and Photonics, 1993, pp. 184–191.

Received 10 October 2014; revised accepted 5 February 2016

doi: 10.18520/cs/v110/i11/2166-2169